

# Scaling violations: Connections between elastic and inelastic hadron scattering in a geometrical approach

P.C. Beggio and M.J. Menon  
*Instituto de Física “Gleb Wataghin”,  
 Universidade Estadual de Campinas, Unicamp,  
 13083-970 Campinas, SP, Brazil*

P. Valin  
*Dépt. de Physique, Université de Montréal,  
 CP. 6128, Succ. Centre-Ville  
 Montréal, Québec, Canada H3C 3J7*

Starting from a short range expansion of the inelastic overlap function, capable of describing quite well the elastic  $pp$  and  $\bar{p}p$  scattering data, we obtain extensions to the inelastic channel, through unitarity and an impact parameter approach. Based on geometrical arguments we infer some characteristics of the elementary hadronic process and this allows an excellent description of the inclusive multiplicity distributions in  $pp$  and  $\bar{p}p$  collisions. With this approach we quantitatively correlate the violations of both geometrical and KNO scaling in an analytical way. The physical picture from both channels is that the geometrical evolution of the hadronic constituents is principally responsible for the energy dependence of the physical quantities rather than the dynamical (elementary) interaction itself.

PACS numbers: 13.85.Hd, 13.65.Ti, 13.85.Dz, 11.80.Fv  
 e-mail: menon@ifi.unicamp.br, fax: 55-19-7885512, phone: (19) 7885530

## Table of Contents

### I. INTRODUCTION

### II. EXPERIMENTAL DATA AND PHENOMENOLOGICAL CONTEXT

- A. Elastic channel
- B. Inelastic channel
- C. Strategies

### III. UNITARITY AND IMPACT PARAMETER PICTURE

- A. Hadronic and elementary multiplicity distributions
- B. Elastic channel input: the BEL  $G_{in}$
- C. Elementary hadronic process in a geometrical picture
  - Analytical relation between multiplicity function and eikonal
  - Elementary multiplicity distribution
  - Power coefficient
- D. Results for the hadronic multiplicity distributions

### IV DISCUSSION

- A. Sensitivity of the parametrizations
  - Changing  $G_{in}$
  - Changing the elementary distribution  $\varphi$
  - Changing the power coefficient  $\gamma$
- B. The multiplicity function and the power assumption
- C. Physical picture

### V. CONCLUSIONS AND FINAL REMARKS

## I. INTRODUCTION

Hadron scattering is presently one of the most intriguing process in high energy particle physics. Unlike the unification scheme which characterizes the electroweak sector of the standard model, some topical aspects of quantum chromodynamics (QCD) remain yet unknown and this has been a great challenge for decades. One point concerns some subtleties emerging from its running coupling constant, which entails that high energy hadronic phenomena have been classified into two wide and nearly incongruous areas, namely, large  $p_T$  or hard processes and low  $p_T$  or soft hadronic physics. From a purely theoretical point of view (QCD), these phenomena are treated through perturbative and non-perturbative approaches respectively, and this renders difficult an unified formalism able to describe the totality of experimental data available on high energy hadronic interactions. The reason is that, despite the successes of perturbative QCD in the description of the hard (inelastic) hadronic scattering and also the successes of non-perturbative QCD in treating static properties of the hadronic systems, the *scattering states in the soft (long range) region* yet remains without a *pure* QCD explanation: Perturbative approaches do not apply and *pure* non-perturbative formalisms are not yet able to predict the bulk of the scattering states.

This soft hadronic physics is associated with the elastic and diffractive scattering, characterized, experimentally, by several physical quantities in both the elastic and inelastic channels, such as elastic differential cross section, total cross section, charged multiplicity distributions, average multiplicities and others [1]. In spite of the long efforts to describe these data through a pure microscopic theory (QCD), our knowledge is still largely phenomenological and also based on a wide class of models and some distinct theoretical concepts, such as Pomeron, Odderon, impact parameter picture, parton and dual models, Monte Carlo approaches and so on.

However, presently, this phenomenological treatment of the soft hadronic physics plays an important role as a source of new theoretical insights and as a strategy in the search for adequate calculational schemes in QCD. The multiple facets associated with this phenomenological scenario have been extensively discussed in the literature and Ref. [2] presents a detailed outlook of the progresses and present status of the area.

In addition to the intrinsic importance of high energy diffractive physics associated with our limited theoretical understanding, a renewed interest in the subject may be seen in the last years. This, in part, is due to the Hera and Tevatron programs, but also to the advent of the next accelerator generation, the Relativistic Heavy Ion Collider (RHIC) and the CERN Large Hadron Collider (LHC). In fact, with these new machines it shall be possible to investigate  $pp$  collisions at center-of-mass energies never reached before in accelerators, allowing comparative studies between  $pp$  and  $\bar{p}p$  scattering at the highest energies, including both hard and soft processes.

Presently, at this “pre-new-era” stage and due to the *lack of an widely accepted unified theoretical treatment of both elastic and inelastic channels*, it may be important to re-investigate *ways of connecting* these channels, looking for new information. Even if the treatment is essentially phenomenological, as explained before, the predictions shall be checked and may contribute with future theoretical (QCD) developments.

To this end, in this work we shall investigate some aspects of both elastic and inelastic  $pp$  and  $\bar{p}p$  scattering in the context of a particular phenomenological approach. Our goal is to obtain simultaneous descriptions of some experimental data from both channels, that is, our primary interest concerns *connections between elastic and inelastic hadron scattering*. Accordingly we shall base our study on one of the most important principle of quantum field theory: Unitarity.

For reasons that will be explained in detail in what follows, our framework is the impact parameter formalism (geometrical approach). At first, under geometrical considerations, we shall not refer to quarks/gluons or partons, but treat hadron-hadron interactions as collisions between composite objects made up by elementary parts, which we shall generically refer as “constituents”. At the end we discuss some possible connections between our results and the framework of QCD. Also, as shall be explained, our starting point is the description of physical quantities that characterize the elastic channel in  $pp$  and  $\bar{p}p$  scattering. We then proceed to consider the inelastic channel through unitarity arguments and in a geometrical approach.

Following other authors [3,4], we shall express the “complex” (overall) hadron- $p$  multiplicity distributions (inelastic channel) in terms of an “elementary” distribution (associated with an elementary process taking place at given impact parameter) and the inelastic overlap function, which is constructed from descriptions of the elastic channel data. The novel aspects concern: (a) quantitative correlation between the *violations* of the Koba-Nielsen-Olesen (KNO) scaling [5] (inelastic channel) and geometrical scaling [6] (elastic channel); (b) introduction of novel parametrizations for the elementary quantities based on geometrical arguments and taking suitable account of the most recent data on *contact interactions*. With this general formalism, in addition to the description of the elastic data (even at large momentum transfers), the hadronic multiplicity distributions may be evaluated and an excellent reproduction of the experimental data on  $pp$  and  $\bar{p}p$  inelastic multiplicities is achieved [7]. We also present predictions at the LHC energies.

The paper is organized as follows. In Sec. II we discuss the underlying phenomenological ideas, the data to be investigated and the strategy assumed. In Sec. III we present the theoretical framework connecting elastic and inelastic channels, the inputs from elastic scattering data, the novel parametrizations for the elementary processes,

the predictions for the hadronic multiplicities distributions and comparison with the experimental data. In Sec. IV we discuss in some detail all the results obtained and the physical and geometrical interpretations. The conclusions and some final remarks are the content of Sec. V.

In what follows we shall represent the main physical quantities associated with hadron-hadron scattering (complex/overall system) by capital letters and those associated with constituent-constituent interactions (elementary process) by lower case.

## II. EXPERIMENTAL DATA AND PHENOMENOLOGICAL CONTEXT

The broad classification in hard, soft (and also semi-hard) processes is based on the momentum transferred in the collision. On the other hand, depending on the physical process involved, high energy hadron scattering may also be classified into elastic and inelastic processes and the later, in diffractive (single and double dissociation) and non diffractive. Concerning *both elastic and inelastic channels*, one of the striking features that emerged from early experiments was the violation of the scaling laws, namely, the geometrical scaling in elastic scattering [6] and the KNO scaling in the inelastic events [5]. For this reason, our main interest in this work is to correlate quantitatively the above scaling violations and to discuss its phenomenological and dynamical aspects. To this end, before we present the underlying formalism and results, we discuss in this section the physical observables to be investigated and the reasons for our choices concerning phenomenology and strategies.

### A. Elastic channel

The differential cross section is the most important physical observable in the elastic channel, since from it other quantities may be obtained, in particular, the integrated elastic cross section,  $\sigma_{el}$ , and the total cross section,  $\sigma_{tot}$  (optical theorem). The violation of the geometrical scaling may be characterized by the increase of the ratio  $\sigma_{el}/\sigma_{tot}$  with the energy at the CERN Intersecting Storage Ring (*ISR*) and at the CERN Super Proton Synchrotron (*SppS*) regions.

The differential cross section yields the elastic hadronic amplitude,  $F(q, s)$ , by

$$\frac{d\sigma}{dq^2} = \pi |F(q, s)|^2 \quad (1)$$

and this amplitude may be expressed in terms of the elastic profile function,  $\Gamma(b, s)$ , by

$$F(q, s) = i \int b db J_0(qb) \Gamma(b, s), \quad (2)$$

where  $b$  is the impact parameter and  $\sqrt{s}$  the center-of-mass energy.

As commented before, despite the bulk of models able to reproduce the differential cross section data at the *ISR*, *SppS* and Tevatron energies [2], an approach based exclusively in QCD is still missing. Obviously due to its *soft* character, a QCD treatment of the elastic scattering should be non-perturbative. Along this line, despite the difficulties, important results have recently been reached through the works by Landshoff, Nachtmann, Simonov, Dosch, Ferreira and Kramer [8,9]. The approach, based on the functional integral representation (QCD) and eikonal approximation, allows to extract a quark-quark profile function  $\gamma(b)$  (impact parameter space) from the gluon gauge-invariant two-point correlation function, determined, for example, from lattice QCD [10]. Through the Fourier transform (analogous to Eq. (2) at the elementary level), the quark-quark scattering amplitude,  $f(q, s)$ , may be obtained:

$$f(q, s) = i \int b db J_0(qb) \gamma(b, s). \quad (3)$$

One possible connection with the hadronic scattering amplitude, Eq. (2), is by means of the Stochastic Vacuum Model (SVM) [9] and some important results have recently been obtained [11]. However, presently, this theoretical framework still depends on some phenomenological inputs. Also, it is able to reproduce only the experimental data in the forward region and/or very small values of the momentum transfer and does not distinguish  $pp$  and  $\bar{p}p$  scattering (dip region), even at *ISR* energies [11].

Another way to obtain the hadronic amplitude from the elementary one is through the Glauber's multiple diffraction theory (MDT) [12] and this plays a central role in our choices concerning phenomenology and strategies as discussed in what follows.

Originally the MDT was applied to hadron-nucleus and nucleus-nucleus collisions [12] and after to hadron-hadron scattering [13]. The topical point which interest us is the allowed general connection between complex quantity (composite object) and elementary quantity (constituents). In the case of hadron-hadron collisions, the connection

between the hadronic amplitude (composite object) and the elementary amplitude (constituents) is also established through the eikonal approximation. In this approach the hadronic profile function, Eq. (2), is expressed by

$$\Gamma(b, s) = 1 - e^{i\chi(b, s)}, \quad (4)$$

where

$$\chi(b, s) = C \int q dq J_0(qb) G_A G_B f \quad (5)$$

is the eikonal function,  $G_{A,B}$  the hadronic form factors,  $f$  the elementary (constituent - constituent) amplitude and  $C$  does not depend on the transferred momentum. The above notation [14] shall be useful for the discussion we are interested in.

In spite of their simplicity, Eqs. (2), (4) and (5) are extremely useful. Recently, with suitable parametrizations for the form factors and with the elementary amplitude (quark-quark) extracted from a parametrization for the gluonic correlator through the functional approach (non-perturbative QCD), Grandel and Weise obtained good descriptions of the differential cross section data for  $pp$  and  $\bar{p}p$  elastic scattering at the  $ISR$  and  $S\bar{p}pS$  energies, but only in the region of small momentum transfer [15]. On the other hand, excellent descriptions of experimental data, including also large momentum transfers, have been obtained in a rather phenomenological context, through suitable parametrizations for  $G_A$ ,  $G_B$  and  $f$  [16]. Moreover, elementary amplitudes obtained through the SVM and the gluonic correlator from lattice QCD have been investigated and also comparisons with empirical analysis and model predictions have been discussed [14,17].

We understand that all these facts indicate that the impact parameter formalism (and the eikonal approximation), connecting the complex (overall) amplitude with the elementary amplitude (constituent-constituent), Eqs. (2), (4) and (5), is a very fruitful and simple approach in the investigation of the elastic hadron scattering. As shown, it seems also to be an adequate bridge between phenomenology and non-perturbative QCD. These conclusions constitute one of the foundations of our approach and, as discussed in what follows, the *extensions to the inelastic channel shall be based on the general idea of connections between overall and elementary quantities in an impact parameter picture.*

## B. Inelastic channel

Concerning scaling in the inelastic channel, the quantity of interest is the hadronic charged particle multiplicity distribution  $P_N$ , normalized in terms of the KNO variable,  $Z = N(s)/\langle N \rangle(s)$ , as

$$\langle N \rangle(s) P_N(Z) \equiv \Phi. \quad (6)$$

The broader distribution observed at the  $S\bar{p}pS$  characterizes the violation of the KNO scaling, namely,  $\Phi = \Phi(Z, s)$ .

As in the case of elastic differential cross section data, a wide class of models describes this behavior, as for example, dual parton [18], fireball [19], two-component models [20], and others. Also, hadronic processes have been extensively treated through Monte Carlo event generators and the Lund parton approach [21–23]. However, we observe that, despite some QCD inspired approaches and good descriptions of some soft processes, all these formalisms and models are concerned *exclusively* with the inelastic channel and this is the topical point that distinguishes our strategy, as discussed in what follows. We shall also return to this subject in Secs. IV and V.

## C. Strategies

Connections between Geometrical and KNO scalings were established a long time ago, by Dias de Deus [6], Lam and Yeung [4]. However, we are interested here in their violations and the central point is: Does one need a new connection when the two phenomena are violated at the  $S\bar{p}pS$  or can the two effects be correlated both phenomenologically and dynamically? We will argue that the latter alternative seems to be prevail. Specifically, our goal is to correlate quantitatively both violations in an analytical way and we shall show that, beginning with a formalism that describes quite well the violation of the Geometrical scaling (elastic channel input), it is possible to extend it and to describe, quantitatively, the violation of the KNO scaling in an analytical way. We stress that this strategy distinguishes our approach from all the other model and theoretical descriptions of elastic or inelastic scattering that treat these interactions separately, in an independent way or in distinct contexts.

Since the connection between *elastic channel*  $\rightarrow$  *inelastic channel* is our primary interest, the approach shall be based in direct analogy with the ideas discussed in Sec. II.A, that is, we consider hadron-hadron collisions as collisions between complex objects, each one composed by a number of more elementary ones. As an extension of the Glauber multiple diffraction theory, which connects hadronic and elementary elastic amplitudes, we shall consider the impact parameter formalism and also express the hadronic multiplicity distribution (complex system) in terms of elementary multiplicity distributions (constituents). The point is to describe a “wide” distribution (hadronic) by superimposing a

number of narrower ones (elementary) [4]. What we shall do here is to infer what these elementary distributions should be, in order to reproduce the experimental data on hadronic distributions and in the context of the impact parameter picture. He hope that, as in the elastic case, these information can contribute to further theoretical developments.

### III. UNITARITY AND IMPACT PARAMETER PICTURE

Unitarity is one of the most important principles in quantum field theory. In the geometrical picture, unitarity correlates the elastic scattering amplitude in the impact parameter  $b$  space,  $\Gamma(b, s)$ , Eq. (2), with the inelastic overlap function,  $G_{in}(b, s)$ , by

$$2Re\Gamma(b, s) = |\Gamma(b, s)|^2 + G_{in}(b, s) \quad (7)$$

which is term-by-term equivalent to [24]

$$G_{tot}(b, s) = G_{el}(b, s) + G_{in}(b, s). \quad (8)$$

For a purely imaginary elastic amplitude in momentum transfer space the profile function  $\Gamma(b, s)$  is real and in the eikonal approximation is expressed by

$$\Gamma(b, s) = 1 - \exp[-\Omega(b, s)], \quad (9)$$

where  $\Omega(b, s) = Im\chi(b, s)$  in Eq. (4). With this,

$$G_{in}(b, s) = 1 - \exp[-2\Omega(b, s)] \equiv \sigma_{in}(b, s) \quad (10)$$

is the probability for an inelastic event to take place at  $b$  and  $s$  and

$$\sigma_{in}(s) = \int d^2\mathbf{b} G_{in}(b, s). \quad (11)$$

In this picture the topological cross section for producing an even number  $N$  of charged particles at CM energy  $\sqrt{s}$  is given by

$$\sigma_N(s) = \int d^2\mathbf{b} \sigma_N(b, s) = \int d^2\mathbf{b} \sigma_{in}(b, s) \left[ \frac{\sigma_N(b, s)}{\sigma_{in}(b, s)} \right] \quad (12)$$

where the quantity in brackets can be interpreted as the probability of producing  $N$  particles at impact parameter  $b$ .

#### A. Hadronic and elementary multiplicity distributions

We now introduce the multiplicity distributions for both an overall and an elementary processes in terms of corresponding KNO variables [5] and also the formal connection between these distributions.

Representing the hadronic (overall) multiplicity distribution by  $\Phi$  and the corresponding KNO variable by

$$Z = \frac{N(s)}{\langle N \rangle(s)} \quad (13)$$

where  $\langle N \rangle(s)$  is the average hadronic multiplicity at  $\sqrt{s}$ , we have in general

$$\Phi = \langle N \rangle(s) \frac{\sigma_N(s)}{\sigma_{in}(s)} = \Phi(Z, s). \quad (14)$$

Now, let  $\langle n \rangle(b, s)$  be the average number of particles produced at  $b$  and  $s$ ,  $\varphi$  the elementary multiplicity distribution and

$$z = \frac{N(s)}{\langle n \rangle(b, s)} \quad (15)$$

a KNO variable associated with the elementary process taking place at  $b$  (and  $s$ ). Then, in general,

$$\varphi = \langle n \rangle(b, s) \frac{\sigma_N(b, s)}{\sigma_{in}(b, s)} = \varphi(z, s). \quad (16)$$

Both distributions are normalized by the usual conditions [3,4]

$$\int_0^\infty \Phi(Z) dZ = 2 = \int_0^\infty \Phi(Z) Z dZ. \quad (17)$$

$$\int_0^\infty \varphi(z) dz = 2 = \int_0^\infty \varphi(z) z dz, \quad (18)$$

The relationship between  $\Phi$  and  $\varphi$  then follows from Eqs. (10-12), (14) and (16):

$$\Phi = \frac{\langle N \rangle (s) \int d^2\mathbf{b} \frac{G_{in}(b,s)}{\langle n \rangle (b,s)} \varphi}{\int d^2\mathbf{b} G_{in}(b,s)}. \quad (19)$$

Now, let us define a *multiplicity function*  $m(b, s)$  by the ratio

$$m(b, s) = \frac{\langle n \rangle (b, s)}{\langle N \rangle (s)}, \quad (20)$$

so that Eq. (19) becomes

$$\Phi = \frac{\int d^2\mathbf{b} \frac{G_{in}(b,s)}{m(b,s)} \varphi\left(\frac{Z}{m(b,s)}\right)}{\int d^2\mathbf{b} G_{in}(b,s)} = \Phi(Z, s). \quad (21)$$

It is well known that connections between KNO and Geometrical scaling may be established if  $m(b, s) = m(b/R(s))$  and also  $G_{in}(b, s) = G_{in}(b/R(s))$  [6], where  $R(s)$  is the “geometrical radius”. In this case  $\Phi(Z, s)$  is only a function of  $Z$ .

The general result (21) means that, once one has parametrizations for  $G_{in}(b, s)$  and the elementary quantities  $\varphi$  (multiplicities distribution) and  $m(b, s)$  (multiplicity function) the overall hadronic multiplicity distribution may be evaluated. In this work we consider  $G_{in}(b, s)$  from analyses of elastic  $pp$  and  $\bar{p}p$  scattering data (taking account of geometrical scaling violation) and infer the elementary quantities based on geometric arguments, as explained in what follows. In so doing, we shall correlate quantitatively the *violations* of both KNO and Geometrical scaling in an analytical way.

### B. Elastic channel input: the BEL $G_{in}$

In the elastic channel, the breaking of Geometrical scaling is quite well described by the BEL behaviour, analytically expressed by the Short Range Expansion of the inelastic overlap function [24,25]

$$G_{in}(b, s) = P(s) \exp\{-b^2/4B(s)\} k(x, s), \quad (22)$$

with  $k$  being expanded in terms of a short-range variable  $x = b \exp\{-(\epsilon b)^2/4B(s)\}$ , i.e.

$$k(x, s) = \sum_{n=0}^N \delta_{2n}(s) \left[ \frac{\epsilon \exp\{1/2\}}{\sqrt{2B(s)}} x \right]^{2n}. \quad (23)$$

The quantity in the bracket of (23) by itself exhibits GS for constant values of  $\epsilon^2 \approx 0.78$ , but  $k(x, s)$  doesn't because of the  $s$ -dependence of  $\delta_{2n}(s)$  and therefore  $G_{in}(b, s)$  doesn't either (also because of  $P(s)$ ). Each term in the bracket of (23) has a maximum value of 1 and the rapid convergence of the series reproduces data for all values of  $-t \in (0, 14)$  GeV<sup>2</sup> with  $N=3$ . For  $k=1=P$ , we recover the Van Hove limit for  $\sigma_{el}/\sigma_{tot}=1-\frac{1}{4(1-\ln 2)} \approx 0.1853$  which is nearly attained at the ISR. The deviation of  $k$  from the constant value of 1, in particular the increase of  $\delta_2(s)$  with increasing  $s$  is responsible for the *Edgier* behaviour of  $G_{in}(b, s)$ , while increasing values of  $P(s)$  and  $B(s)$  make the proton *Blacker* and *Larger* respectively (BEL behavior of the inelastic overlap function).

Excellent agreement with experimental data on  $pp$  and  $\bar{p}p$  elastic scattering is achieved [25] for the following parametrizations in terms of the Froissart-like variable  $y = \ln^2(s/s_0)$  with  $s_0 = 100$  GeV<sup>2</sup>

$$P(s) = \frac{0.908 + 0.027y}{1 + 0.027y}, \quad \delta_2(s) = 0.115 + 0.00094y \quad (24)$$

$B(s) = 6.64 + 0.044y$   
and  $\delta_4$  determined from  $\delta_2$  in some models [26] by  $\delta_4 = \delta_2^2/4$ .

### C. Elementary hadronic process in a geometrical picture

We now turn to the discussion of the *elementary hadronic process*, characterized by  $\varphi$  and  $m$  in Eq. (21). By construction, these quantities are associated to collisions of strongly interacting hadronic constituents. As commented before, due to the success of the geometrical models in the investigation of *elastic* hadron scattering (for example, the above BEL approach) and the presently lack of a *pure* QCD approach and/or Monte Carlo models to the subject (elastic/soft scattering states), we shall discuss what an *elementary hadronic* process could be in the geometrical framework and in an analytical way. Our arguments are as follows.

In the geometrical approach an elementary process is a process occurring at a given impact parameter. Concerning *contact interactions*, experimental information is *only available from lepton-lepton collisions*, which is a process occurring in a unique angular momentum state and therefore also at a given impact parameter (zero in this case). Although *these processes can not be the same as collisions between hadrons constituents*, it is reasonable, from the geometrical point of view, to think that *some characteristics of both processes could be similar*. The point is to find out or infer what they could be.

For these reasons we shall consider the experimental data available on  $e^+e^-$  collisions as a possible source of (limited) geometrical information concerning elementary hadronic interactions (at given impact parameter). We do not pretend to look for connections between  $e^+e^-$  annihilations and  $pp$  and  $\bar{p}p$  collisions but to extract from the former processes suitable information that allows the construction of the hadronic multiplicities (and the connections with the corresponding elastic amplitude) in an *analytical way and in the geometrical context*. This may be achieved for both  $\varphi$  and  $m$  in Eq. (21) through the following procedure.

- Analytical relation between multiplicity function and eikonal

First, in order to connect the multiplicity function  $m(b, s)$  and the eikonal  $\Omega(b, s)$  [3,4] (and so  $G_{in}(b, s)$  by Eq. (10)) in an *analytical way*, let us consider the very simple assumption that the *average multiplicity at given impact parameter* depends on the center-of-mass energy in the form of a general power law

$$\langle n \rangle (b \text{ fixed}, s) \propto E_{CM}^\gamma. \quad (25)$$

We shall discuss this assumption in detail in Sec. IV.B..

Now, from Eqs. (10) and (11),  $\exp\{-2\Omega(b, s)\}$  is the transmission coefficient, i.e. the probability of having no interaction at a given impact parameter, and therefore  $\Omega$  should be proportional to the thickness of the target, or as first approximation, to the energy  $E_{CM}$  that can be deposited at  $b$  for particle production at a given  $s$ . By Eq. (25) this implies

$$\langle n \rangle (b, s) \propto \Omega^\gamma(b, s). \quad (26)$$

Comparison of Eqs. (20) and (26) allows us to correlate the multiplicity function  $m(b, s)$  with the eikonal through a non-factorizing relation (in  $b$  and  $s$ ):

$$m(b, s) = \xi(s)\Omega^\gamma(b, s), \quad (27)$$

with  $\xi(s)$  being determined by the normalization condition of the overall multiplicity distribution, Eq. (18). With this, Eq. (21) becomes

$$\Phi = \frac{\int d^2\mathbf{b} \frac{G_{in}(b, s)}{\xi\Omega^\gamma(b, s)} \varphi\left(\frac{Z}{\xi\Omega^\gamma(b, s)}\right)}{\int d^2\mathbf{b} G_{in}(b, s)} \quad (28)$$

where

$$\xi(s) = \frac{\int db^2 G_{in}(b, s)}{\int db^2 G_{in}(b, s)\Omega^\gamma(b, s)}. \quad (29)$$

Once the above *analytical connection* is assumed, the elementary hadronic process is now characterized by only two quantities, namely, the elementary distribution  $\varphi$  and the power coefficient  $\gamma$ . We proceed with the determination of these quantities through quantitative analyses of  $e^+e^-$  data and under the following arguments.

- Elementary multiplicity distribution

Because the elementary process occurs at a given impact parameter, its elementary structure suggests that it should scale in the KNO sense. Now, since experimental information on  $e^+e^-$  multiplicity distributions shows agreement with this scaling [27], we shall base our parametrization for  $\varphi$  just on these data. In particular, it is sufficient to assume a gamma distribution (one free parameter), normalized according to Eq. (17),

$$\varphi(z) = 2 \frac{K^K}{\Gamma(K)} z^{K-1} \exp\{-Kz\}. \quad (30)$$

Fit to the most recent data, covering the interval  $22.0 \text{ GeV} \leq \sqrt{s} \leq 161 \text{ GeV}$  [27,28] furnished  $K = 10.775 \pm 0.064$  with  $\chi^2/N_{DF} = 508/195 = 2.61$  and the result is shown in Fig. 1.

Concerning this fit, we verified that data at 29 and 56 GeV make the highest contributions in terms of  $\chi^2$  values. For example, if the former data are excluded we obtain  $K = 10.62$  and  $\chi^2/N_{DF} = 414/181 = 2.29$  and if both sets are excluded then  $K = 10.88$  and  $\chi^2/N_{DF} = 286/162 = 1.77$ . For comparison we recall that the DELPHI fit through a negative binomial distribution to data at only 91 GeV gives  $\chi^2/N_{DF} = 80/34 = 2.35$  (and  $\chi^2/N_{DF} = 43/33 = 1.30$  through a modified negative binomial distribution) [27]. However, we also verified that the above two values for  $K$  are not so sensitive in the final result concerning the hadronic multiplicity distribution, which is our goal (we shall return to this point in Sec. IV.A). For this reason and since we are only looking for experimental information that could represent contact interactions (geometrical point of view) we consider our first result shown in Fig. 1 as the representative one.

- Power coefficient

Finally, following Eq. (25), we consider fits to the  $e^+e^-$  average multiplicity through the general power law

$$\langle n \rangle_{e^+e^-} = A[\sqrt{s}]^\gamma. \quad (31)$$

We collected experimental data at center-of-mass energies above resonances and thresholds and also the most recent data at the highest energies, covering the interval  $5.1 \text{ GeV} \leq \sqrt{s} \leq 183 \text{ GeV}$  [28,29]. Fitting to Eq. (31) yields  $A=2.09 \pm 0.02$ ,

$$\gamma = 0.516 \pm 0.002 \quad (32)$$

with  $\chi^2/N_{DF} = 409/46 = 8.89$  and the result is shown in Fig. 2. We observe that this parametrization deviates from the data above  $\sqrt{s} \sim 100 \text{ GeV}$  and this contributes to the high  $\chi^2$  value. However, as commented before, we do not expect that  $e^+e^-$  annihilation exactly represent the collisions between hadrons constituents. The power law is a form which allows an *analytical* and simple connection between the multiplicity function and the eikonal as expressed by Eq. (27). In Sec. IV.B we present a detailed discussion concerning this power assumption and in Sec. IV.A and IV.C, we discuss the physical meaning of the differences between our parametrization and the experimental data on  $\langle n \rangle_{e^+e^-}$ .

#### D. Results for the hadronic multiplicities distributions

With the above results we are now able to predict the hadronic inelastic multiplicity distribution  $\Phi(Z, s)$ , Eqs. (28, 29), without free parameters:  $G_{in}(b, s)$  (and  $\Omega(b, s)$ ) comes from analysis of the elastic scattering data (Eq. (10) and (22-24));  $\varphi(z)$  and  $\gamma$  from fits to  $e^+e^-$  data, Eq. (30) and (31-32) respectively.

We express  $\Phi$  in terms of the scaling variable  $Z' = N'/\langle N' \rangle$  where  $\langle N' \rangle = N(s) - N_0$  with  $N_0=0.9$  leading charges removed. It is well known [30] that such a subtraction improve the KNO curves for all measured data below the  $S\bar{p}pS$  Collider with the above value of  $N_0$ . This is completely equivalent to the Wroblewski [31] relation for the dispersion  $D = \sqrt{N^2 - \langle N \rangle^2} = 0.594 [\langle N \rangle - N_0]$  with the same value of  $N_0$ . Values of  $N_0$  around 1 and the numerical value of the  $D$  vs  $N$  can be found by parton model arguments [32] for valence quark distributions.

The predictions for  $pp$  scattering at ISR energies and  $\bar{p}p$  at 546 GeV are shown in Figs. (3) and (4), respectively, together with the experimental data [33,34]. The theoretical curves present excellent agreement with all the data, showing a slow evolution with the energy at ISR for large  $Z'$  and reproducing the KNO violations for large  $Z'$  values at 546 GeV. In Fig. (4) is also shown the predictions at 14 TeV (LHC).

### IV DISCUSSION

In the last section we obtained a quantitative correlation between the violations of both KNO and geometrical scaling. In the framework of the impact parameter picture, Sec. III.A, we only used four inputs, three parametrizations from fits to experimental data and one geometrical assumption, namely,

1.  $G_{in}(b, s)$  from fits to elastic scattering data (BEL behavior);
2.  $\varphi(z)$  from fit to  $e^+e^-$  multiplicity distribution data;
3. The geometrical assumption (27) concerning the multiplicity function  $m(b, s)$ ;
4. The power coefficient  $\gamma$ , from fit to  $e^+e^-$  average multiplicities data.

In this section, we first investigate the sensitivity of each parametrization from fits to the experimental data in the output of interest, namely, the hadronic multiplicity distribution. Then, we discuss in some detail the geometrical assumption concerning the multiplicity function and the power law. Finally, based on this study, we outline the physical picture associated with all the results from both geometrical/phenomenological and QCD point of views.

### A. Sensitivity of the parametrizations

First we observe that the power coefficient  $\gamma$  in Eqs. (28-29) could, formally, be considered as a free parameter in a direct fit to the data on the hadronic multiplicity distributions and, in this case, it would not be necessary to take account of the  $e^+e^-$  average multiplicity data. This, however, leads to a strong correlation between  $\gamma$  and the other two inputs,  $G_{in}(b, s)$  and  $\varphi(z)$ . On the other hand, with our procedure, the values and behaviours of the three inputs,  $G_{in}$ ,  $\varphi$  and  $\gamma$ , are roughly uncorrelated and this allows tests of the inputs by fixing two of them and changing the third. In what follows we perform this kind of analysis, beginning allways with the results obtained in the last section and considering, separately, a change in each one of the inputs. Since we are interested in the scaling violation we shall base this study in the results for the hadronic multiplicity distribution only at the collider energy.

#### • Changing $G_{in}$

Among the wide class of models for  $G_{in}$  [2], we shall consider a multiple diffraction model (MDM) and also the traditional approach by Chou and Yang, as a class of geometrical model (GM). The reason is based on the discussion in Sec. II.A. Also, as we shall show in Sec. IV.C, these models allows a suitable connection with the interpretations that can be inferred from our general approach.

##### - Multiple diffraction model (MDM)

This class of models is characterized by each particular choice of parametrizations for the physical quantities in Eq. (5), namely, form factors,  $G_{A,B}$  and elementary scattering amplitude  $f$  [14]. In particular, Menon and Pimentel obtained a good description of the experimental data o  $pp$  and  $\bar{p}p$  elastic scattering, above  $\sqrt{s} = 10 \text{ GeV}$  through the following choices citemenonpimentel:

$$G_A(q) = G_B(q) = \frac{1}{(1 + \frac{q^2}{\alpha^2})(1 + \frac{q^2}{\beta^2})}, \quad (33)$$

$$f(q) = \frac{i[1 - (q^2/a^2)]}{[1 + (q^2/a^2)^2]}. \quad (34)$$

The parameters  $\alpha^2$  and  $\beta^2$  are fixed and the dependence on the energy is contained in the other two parameters:

$$C(s) = \xi_3 \exp\{\xi_4 [\ln(s)]^2\}, \quad (35)$$

$$\alpha_{(s)}^2 = \xi_1 [\ln(s)]^{\xi_2}, \quad (36)$$

where  $\xi_i$ ,  $i = 1, 2, 3, 4$  are real constants. The reason for these choices and physical interpretaions are extensively discussed in [36]. With these parametrizations the opacity function,

$$\Omega(b, s) = \text{Im}\chi(b, s), \quad (37)$$

is analytically determined and then the inelastic overlap function through Eq. (10).

##### - Geometrical model (GM)

In the geometrical approach by Chou and Yang, the essential ingredient is the convolution of form factors in the impact parameter space [37]. However, in the context of the multiple diffraction theory, it can also be specified by the following choices [14]:

$$G_A(q) = G_B(q) = \frac{1}{2\pi[1 + (\frac{q^2}{\mu^2})]^2}, \quad (38)$$

$$f = 1. \quad (39)$$

In Ref. [38] the parameters  $\mu$  and  $C$  were determined through fits to elastic  $pp$  data at  $\sqrt{s} = 23.5 \text{ GeV}$  and  $\bar{p}p$  at  $546 \text{ GeV}$ . Following the authors, we consider the parametrizations

$$C(s) = a_1 + a_2 \ln s, \quad \frac{1}{\mu^2(s)} = b_1 + b_2 \ln s. \quad (40)$$

With the above double pole parametrization for the form factors, the opacity, Eq. (5), is analytically determined and so the inelastic overlap function, Eq. (10).

#### - Results

The results for the inelastic overlap function at  $546 \text{ GeV}$  are shown in Fig. 5, from both the MDM and the GM, together with the BEL  $G_{in}$  for comparison. In what follows, we shall use the following notation for these parametrizations  $G_{in}^{MDM}$ ,  $G_{in}^{GM}$ , and  $G_{in}^{BEL}$ , respectively.

We then calculate the hadronic multiplicity distribution, Eqs. (28-29), at this energy, by fixing both  $\gamma = 0.516$ , Eq. (32), and the gamma parametrization for the elementary multiplicity  $\varphi(z)$ , Eq. (30), and using  $G_{in}^{MDM}$  and  $G_{in}^{GM}$ . The results are displayed in Fig. 6 together with that obtained with  $G_{in}^{BEL}$  (Fig. 4) for comparison.

We observe that, for central collisions (small  $b$ ),  $G_{in}^{BEL}$  and  $G_{in}^{GM}$  are very similar, but  $G_{in}^{MDM}$  has higher values (Fig. 5a). This leads to the differences in  $\phi(Z')$  at high multiplicities, as can be seen in Fig. 6. In the same way, the differences between  $G_{in}^{MDM}$ ,  $G_{in}^{GM}$ , and  $G_{in}^{BEL}$  at large  $b$  (Fig. 5b) originate the differences in  $\phi(Z')$  at small multiplicities. In all the cases the physical picture is that large multiplicities (large  $Z'$ ) occur for small impact parameters while grazing collisions (large  $b$ ) lead to small multiplicities, as one would have naively expected.

An important conclusion is that, with  $\gamma$  and  $\varphi(z)$  fixed, the hadronic multiplicity distributions obtained with  $G_{in}^{MDM}$ ,  $G_{in}^{GM}$ , and  $G_{in}^{BEL}$  reproduce the experimental data quite well. We shall return to this point in Sec. IV.C.

#### • Changing the elementary distribution $\varphi$

As a pedagogical exercise, we shall consider only an early parametrization introduced by Barshay and Yamaguchi [39],

$$\varphi_{BY}(z) = \frac{81\pi^2}{64} z^3 \exp\left\{-\frac{9\pi}{16} z^2\right\}. \quad (41)$$

This function was used in the analysis of  $e^+e^-$  multiplicity distributions at lower energies and, as can be seen in Fig 7, does not reproduce the data at higher energies as well as the gamma parametrization.

As before, we now proceed by fixing both  $\gamma = 0.516$  and  $G_{in}^{BEL}$  and using the above parametrization for the elementary distribution. The result for the hadronic multiplicity distribution at  $546 \text{ GeV}$  is shown in Fig. 8, together with the result obtained with the gamma parametrization for the elementary process (Fig. 4). The broader width of  $\varphi_{BY}(z)$  as compared with that of the gamma distribution, is directly reflected in the hadronic multiplicity. Despite the differences between the two parametrizations for the elementary process the final result for the hadronic distribution with  $\varphi_{BY}$  can yet be considered as a reasonable reproduction of the experimental data.

#### • Changing the power coefficient $\gamma$

Finally, we consider different parametrizations for the  $e^+e^-$  average multiplicity data in the interval  $5.1 \leq \sqrt{s} \leq 183 \text{ GeV}$ , but under the assumption of the power dependence. We shall discuss this assumption in the next section.

First we consider the naive parametrization based on the thermodynamic model (see next section)

$$\langle n \rangle_{e^+e^-} = 2.20[\sqrt{s}]^{0.500}. \quad (42)$$

For the above ensemble of data one obtains  $\chi^2/DOF = 209/48 = 4.35$ .

Second, and more importantly, we shall investigate the effect of the data at the highest energies, which are not reproduced by our original parametrization, as can be seen in Fig. 2. To this end, we consider only the data above  $10 \text{ GeV}$  (25 data points) and the general power law parametrization. With this procedure we obtained

$$\langle n \rangle_{e^+e^-} = 3.46[\sqrt{s}]^{0.396 \pm 0.008}. \quad (43)$$

with  $\chi^2/DOF = 27/23 = 1.7$ .

The result is displayed in Fig. 9 together with Eq. (42) and our original parametrization, Eqs. (31-32). We observe that, concerning  $e^+e^-$  average multiplicity Eq. (43) brings information from data at high energies (roughly above  $50$

GeV), while the original parametrization, Eqs. (31-32) is in agreement with data at smaller energies (below  $\sim 100$  GeV) and the same is true for the parametrization with Eq. (42).

As before, we now calculate the corresponding hadronic multiplicity distribution by fixing both the gamma parametrization for the elementary distribution, Eq. (30), and the  $G_{in}^{BEL}$ , Eqs. (22-24), and considering the three parametrizations for the average multiplicity, Eqs. (31-32), (42) and (43). The results at 546 GeV are shown in Fig. 10.

We conclude that, in the context of our approach with the fixed inputs  $G_{in}^{BEL}$  and gamma parametrization for  $\varphi(z)$ , the information from the  $e^+e^-$  average multiplicities at high energies with the power-law does not reproduce the hadronic multiplicity distribution. That is, the elementary average multiplicity distributions in hadronic interactions must deviate from the  $\langle n \rangle_{e^+e^-}(s)$  as the energy increases, roughly above  $\sim 50 - 100$  GeV. We shall discuss the physical interpretations of this result in Sec. IV.C.

## B. The multiplicity function and the power assumption

We now turn to the discussion of a crucial assumption in our approach, namely, that the *elementary* average multiplicity at fixed impact parameter collisions grows as a power of the center-of-mass energy. To this end we shall first briefly recall some aspects of the power-law in hadron-hadron and  $e^+e^-$  collisions, both in experiment and theory, and after, based on these ideas, we shall present a discussion concerning the use of this assumption in our approach and also the meaning of the multiplicity function.

From the early sixties cosmic ray results on extensive air showers, at energies  $E_{lab} < 10^6 - 10^7$  GeV, led to empirical fits of the type  $\langle N \rangle \propto E_{lab}^{1/4} \propto [\sqrt{s}]^{1/2}$  (see [40] for a review). A general power law with the exponent as a free parameter was used a long time ago, in order to allow analytical connections in analysis of cosmic ray data [41]. Also, in the beginning of sixties, these investigations introduced the concept of inelasticity [40]. This comes from the observation that the energy effectively available for particle production could not be identified with the c.m. energy, as believed before 1953 (Wataghin, Fermi, Landau), but only with a fraction of it:

$$W = k\sqrt{s}. \quad (44)$$

The remained  $(1 - k)\sqrt{s}$  was associated with the early named “isobar” system, presently known as leading particle.

From the theoretical side, the power dependence emerged in the context of statistical models (Fermi, Pomeranchuk) and hydrodynamical models (Heisenberg, Ladau) [40]. For example, taking account of the inelasticity, in the Landau model, the fact that the averaged multiplicity is proportional to the total entropy leads to the result [42]

$$\langle N \rangle \propto k^{3/4} [\sqrt{s}]^{1/2}. \quad (45)$$

Dependences on  $s^{1/2}$  is characteristic of the Heisenberg and Pomeranchuk models and even  $s^{1/8}$  appears in the Landau model, when viscosity is taken into account [40]. In the context of thermodynamic models, a universal formula was discovered for proton targets and for energies below  $\sim 50$  GeV: Data including  $\gamma, \pi, N$  and  $p$  collisions with  $p$  were quite well reproduced by  $\langle N \rangle = 1.75 s^{1/4}$  [43]. Concerning  $e^+e^-$  data on average multiplicity this model suggested  $\langle n \rangle = 1.5 s^{3/8}$  and pure fits to low energy data furnished  $\langle n \rangle = (2.2 \pm 0.1)s^{0.25 \pm 0.01}$ , and also  $\langle n \rangle = (1.73 \pm 0.03)s^{0.34 \pm 0.01}$  [44,45]. Moreover, the power-law, with the exponent 1/4, was successfully used in the context of the parton model, either connecting KNO and Bjorken scaling [46] or treating directly the violation of the KNO scaling [32].

The power-law may also appear under more general arguments. For example, suppose that an intermediate state (fireball) of invariant mass  $M \propto \sqrt{s}$  decays into two systems each of invariant mass  $M_1 = M/c$ , where  $c$  is a constant. Suppose also that similar processes continue through some steps (successive cluster production) until the masses reach a value  $M_0$  (some minimum resonance mass). It is easy to show that the final multiplicity reads [32]

$$n \propto [\sqrt{s}]^{\ln 2 / \ln c}. \quad (46)$$

For example for  $c = 4 \rightarrow n \propto s^{1/4}$ . The exponent  $\gamma$  (our notation) may be inferred from  $c = 2^{1/\gamma}$ , so that higher  $\gamma$  values imply in higher splitted masses in each step (for  $\gamma = 0.516 \rightarrow c \sim 3.8$ ).

Based on the above review, we see that the power-law is characteristic of several analysis of experimental data on hadron-hadron and  $e^+e^-$  collisions and also several theoretical approaches and models. Now we shall discuss this law in the context of our approach.

First let us stress that in our formalism this assumption concerns an *elementary* hadronic process taking place at *fixed impact parameter*  $b$ . Thus, it does not pretend to represent the average hadronic multiplicity  $\langle N(s) \rangle$ . Also, we used  $e^+e^-$  data only as a possible source of information on contact interactions (fixed  $b$ ) and therefore the power assumption does not pretend to represent the average multiplicity in  $e^+e^-$  collisions. This is a subtle point in our approach and we would like to discuss it in some detail.

The main reason for the power assumption was to obtain an analytical and simple connection between the multiplicity function  $m(b, s)$  and the eikonal, Eq. (27), which allows the general analytical connection between the elastic and inelastic channels. Since it is typical of several kind of collisions, as reviewed above, it is not unreasonable that it could represent an elementary hadronic process taking place at fixed impact parameter. Just for its elementary character (at given  $b$ ), there seems also to be no reason to include any inelasticity effect (leading particle) in the basic assumption represented by Eq. (25). That is, it seems reasonable that  $\langle n \rangle (b \text{ fixed}, s)$  may be just proportional only to  $E_{CM}^\gamma$ .

The multiplicity function  $m(b, s)$ , as defined by Eq. (20), connects the hadronic and elementary (at given  $b$ ) average multiplicities. With the power assumption and the geometrical arguments of Sec. II.C,  $m(b, s)$  may be expressed in terms of the eikonal and the power coefficient  $\gamma$ . The subtle point in our approach is that, since by definition  $m(b, s)$  is proportional also to the average elementary multiplicity at given  $b$ , the coefficient  $\gamma$  was determined by fit to data available on contact interactions. In this sense, the model “imposes” the power-law and the  $e^+e^-$  data are supposed to provide the limited, but possible, information on contact interactions.

These considerations may allow to infer a distinction between  $e^+e^-$  average multiplicity and what this quantity could be in an elementary hadronic process. Specifically, we showed in Sec. IV.A that data on the average multiplicity in  $e^+e^-$  collisions, presently available above 5 GeV, can not be reproduced by the power-law. For example, a second degree polynomial in  $\ln s$  gives a quite good fit to all the data above 5 GeV:

$$\langle n \rangle_{e^+e^-}(s) = 0.0434 + 0.775 \ln s + 0.168 \ln^2 s \quad (47)$$

with  $\chi^2/DOF = 145/45 = 3.2$ . However, besides this parametrization does not allow the analytical connection with the eikonal, we showed that, with the power-law, the behavior of  $\langle n \rangle_{e^+e^-}(s)$  at energies above  $\sim 50$  GeV does not lead to the description of the hadronic multiplicity distribution. In other words, in the context of our approach, the increase of the elementary average multiplicity with energy in hadronic collisions must be faster than that observed in  $e^+e^-$  collisions. This is not the case at lower energies, since the power-law with  $\gamma = 0.516$  gives a satisfactory description of the  $e^+e^-$  data. In the next section we discuss the physical interpretations associated with these observations.

### C. Physical picture

Based on the results of Secs. II and III, we now discuss the physical picture associated with the scaling violations, specifically, with the evolution of the hadronic multiplicity distribution  $\Phi(Z')$  from the ISR to the collider and LHC energies, Figs. 3 and 4.

From Eq. (21) the hadronic multiplicity  $\Phi$  is constructed in terms of  $G_{in}$  and the elementary quantities  $\varphi$  and  $m$ . In our approach,  $\varphi$  scales and so does not depend on the energy. The multiplicity function  $m(b, s)$  is connected with  $G_{in}$  through Eqs. (10) and (27),

$$m(b, s) = \xi(s) \{ \ln[1 - G_{in}(s, b)] \}^\gamma, \quad (48)$$

where  $\xi$  comes from the normalization condition (29). Both  $\xi(s)$  and  $m(b, s)$  depend on the power coefficient  $\gamma$ , which is a constant determined from the fit through Eq. (31). Therefore, the evolution of the hadronic distribution with energy comes directly from  $G_{in}(b, s)$  and depends also on the value of the exponent  $\gamma$ . This exponent, in turns, comes from the elementary average multiplicity dependence with the energy, Eq. (31), and therefore is associated with the *effective* number of colliding constituents in the hadronic process.

Based on the above observations, the physical picture that emerges is that the energy evolution of the hadronic multiplicity distribution is correctly reproduced by changing only the overlap function, without tampering with the underlying more elementary process ( $\varphi$ ). The geometrical evolution of the constituents of the hadron is responsible for the energy dependence and not the dynamical interaction itself. This is what one would expect if the underlying interaction is unique (QCD) but the relative importance of the constituents involved in collisions changes with energy (indicated by the exponent  $\gamma$ ).

We showed that with the power assumption, the information from  $e^+e^-$  data above, say,  $\sim 100$  GeV leads to an underestimation of the hadronic multiplicity distribution (Fig. 10). This means that the average multiplicity in an elementary hadronic process must increase with energy faster than that associated with  $e^+e^-$  collisions. This result seems quite reasonable since, in a QCD guided approach, we expect different contributions from gluons/quarks interactions than those associated with lepton-lepton collisions. As the average multiplicity increases, the relevance of the original parton decreases, so that at high energies  $e^+e^-$  can serve as a good first guide to quark-quark, quark-gluon and gluon-gluon multiplicity distributions. In a parton model (following QCD), this effect above  $\sim 100$  GeV may be interpreted as the onset of gluons interactions [32]. The faster increase represented by our power-law with  $\gamma = 0.516$  (Fig. 2) may be attributed to the fully development of the gluonic structure, rather than the quark (valence) structure.

These “microscopic” interpretations are also directly associated with the BEL behavior, since its origin may be traced either to gluon interactions in the eikonal formalism [47,48], or to the increased size of spot scattering in the overlap function formalism [49].

As commented before, a novel aspect of this work concerns the simultaneous treatment of both the elastic and inelastic channels. Specifically, we started from elastic channel descriptions ( $pp$  and  $\bar{p}p$  differential cross sections) and extended the results to the inelastic channel (multiplicity distributions). In this sense, we expect that the physical picture from both channels should be the same. Besides the microscopic interpretation associated with the BEL  $G_{in}(b, s)$ , even if we consider the naive models represented by the MDM and the GM, discussed in Sec. IV.A, the same scenario emerges. In fact, in both models the elementary interaction, represented by the elementary elastic amplitude  $f(q, s)$ , does not depend on the energy, Eqs. (34) and (39). The energy dependence is associated with the form factor  $G(q, s)$  and the “absorption constant”  $C(s)$ . The former, through the associated radius,

$$R^2(s) = -6 \frac{dG}{dq^2} \Big|_{q^2=0}, \quad (49)$$

describes the expansion effect (geometry). The latter is associated with absorption (blackning) in the context of the geometrical (Chou-Yang) model and to the relevant number on constituents in the context of the multiple diffraction theory [12]. herefore, we also conclude that the elementary interaction is unique (does not depend on the energy), but the geometrical evolution of the constituents and its relevant number in collisions changes as the energy increases.

## V. CONCLUSIONS AND FINAL REMARKS

The underlying theory of the hadronic phenomena is QCD. As commented in Secs. I and II, despite all its successes, the theory has presently some limited efficiency in the treatment of soft hadronic processes, mainly related with unified descriptions of physical quantities from *both* elastic and inelastic channels. Moreover, some QCD approaches are based in extensive Monte Carlo calculations and concerning this point, we understand that, although these techniques represent a powerfull tool for experimentalists, it is questionable if they could really be the adequate and final scenario for a theoretical understand of the hadronic interactions, mainly if we think in connections with first principles of QCD.

At this stage, it seems that phenomenology must play an important role to bridge the gap, or, at least, to indicate or suggest some suitable calculational schemes for further theoretical developments. On the other hand, all the phenomenological approaches presently available, have also very limited intervals of validity and efficiency in the treatment of hadronic processes at high energies. One of the serious limitations of the geometrical approach is the difficulty to directly connect its relative efficiency with the well established microscopic ideas (QCD). However, it has not been proved that this direct connection can not be obtained.

In this work, making use of the unitarity principle and in the context of a geometrical picture, we obtained analytical connections between physical quantities from both elastic and inelastic channels. In particular we correlated quantitatively the violations of the geometrical and KNO scalings in an analytical way. The physical picture that emerges from both channels, for  $pp$  and  $\bar{p}p$  collisions above  $\sim 10 \text{ GeV}$  is the following. The dependence of the physical quantities with the energy (elastic differential cross section and inelastic multiplicity distributions) is associated with the geometrical evolution of the constituents and the relative importance of the constituents involved in the collisions. The underlying elementary process or interaction does not change with the energy. This is in agreement with what could be expected from QCD.

With this kind of approach the correct information extracted from the elastic channel is fundamental. Our prediction at LHC energies was based on extrapolations from analysis at lower energies and so has a limited character. This observation, and obviously other considerations regarding different models, point out to the importance of complete measurements of physical quantities associated with the elastic channel at the LHC, that is not only total cross sections but also the  $\rho$  parameter and differential cross sections at large momentum transfer.

Based on the limitations referred to in this section, we do not pretend that the forms we inferred for the hadronic constituent-constituent collisions, multiplicity distribution and average multiplicity, are a conclusive solution. However, we hope that, at least, they can bring new information on what some aspects of an elementary hadronic process could be.

## ACKNOWLEDGEMENTS

Thanks are due to Pierre St. Hilaire. P.C.B. and M.J.M. are thankful to CNPq and FAPESP ( Proc. N. 1998/2249-4) for financial support.

- 
- [1] E. Leader and E. Predazzi, *An introduction to gauge theories and modern particle physics* (Cambridge University Press, Cambridge, 1996), Vols. 1 and 2.
  - [2] *Proceedings of the First International Conference on Elastic and Diffractive Scattering*, Blois, France, 1985, edited by B. Nicolescu (Editions Frontières, Gif-sur-Yvette, 1986); *Proceedings of the Second International Conference on Elastic and Diffractive Scattering*, New York, New York, 1987, edited by K. Goulianos (Editions Frontières, Gif-sur-Yvette, 1988); *Elastic and Diffractive Scattering*, Proceeding of the Third International Conference, Evanston, Illinois, 1989, edited by M. M. Block and A. White [Nucl. Phys. B (Proc. Suppl.) **12** (1990)]; *Proceedings of the Fourth International Conference on Elastic and Diffractive Scattering*, Elba, Italy, 1991, edited by F. Cervelli and S. Zucchelli [Nucl. Phys. B (Proc. Suppl.) **25** (1992)]; *Proceedings of the Vth International Conference on Elastic and Diffractive Scattering*, Brown University, Providence, RI, 1993, edited by H. M. Fried, K. Kang, and C-I Tan (World Scientific, Singapore, 1994); *Frontiers in Strong Interactions*, edited by P. Chiappetta, M. Haguenaue, and J. Trần Thanh Vân (Editions Frontières, Gif-sur-Yvette, 1996).
  - [3] S. Barshay, Phys. Lett. B **116**, 193 (1982); Phys. Rev. Lett. **49**, 1609 (1982).
  - [4] C.S. Lam and P.S. Yeung, Phys. Lett. B **119**, 445 (1982).
  - [5] Z. Koba, H.B. Nielsen and P. Olesen, Nucl. Phys. **B40**, 317 (1972).
  - [6] J. Dias de Deus, Nucl. Phys. **B59**, 231 (1973).
  - [7] P.C. Boggio, M.J. Menon and P. Valin, in *Relatório da X Reunião de Trabalho sobre Interações Hadrônicas*, edited by Y. Hama *et al.* (Instituto de Física, USP, São Paulo, 1999) p. 62.
  - [8] P. Landshoff and O. Nachtmann, Z. Phys. C **35**, 405 (1987); O. Nachtmann, Ann. Phys. (N.Y.) **209**, 436 (1991).
  - [9] H.G. Dosch, Phys. Lett. B **190**, 177 (1987); H.G. Dosch and Yu. A. Simonov, *ibid.* **205**, 339 (1988); A. Krämer and H.G. Dosch, Phys. Lett. B **252**, 669 (1990); H.G. Dosch, E. Ferreira, and A. Krämer, Phys. Rev. D **50**, 1992 (1994).
  - [10] A. Di Giacomo, E. Meggiolaro, and H. Panagopoulos, Nucl. Phys. **B483**, 371 (1997).
  - [11] E. Ferreira, and F. Pereira, Phys. Rev. D **55**, 130 (1997); E.R. Berger, Nucl. Phys. Proc. Suppl. **74**, 96 (1999); E.R. Berger, and O. Nachtmann, Eur. Phys. J. C **7**, 459 (1999).
  - [12] R.J. Glauber, in *Lectures in Theoretical Physics*, edited by W. E. Britten *et al.* (Interscience, New York, 1959) Vol. I, p. 315; W. Czyż and L.C. Maximom, Ann. Phys. (N.Y.) **52**, 59 (1969); V. Franco and G.K. Varma, Phys. Rev. C **18**, 349, (1978).
  - [13] R.J. Glauber and J. Velasco, Phys. Lett. B **147**, 380 (1984); in *Proceedings of the Second International Conference on Elastic and Diffractive Scattering* [2], p. 219.
  - [14] M.J. Menon, Phys. Rev. D **48**, 2007 (1993); **51**, 1427(E) (1995).
  - [15] U. Grandel and W. Weise, Phys. Lett. B **356**, 567 (1995).
  - [16] C. Furget, M. Buenerd, and P. Valin, Z. Phys. C **47**, 377 (1990); J. Pumplin, Phys. Lett. B **289**, 449 (1992); M.J. Menon, in *Proceedings of the Fourth International Conference on Elastic and Diffractive Scattering* [2], p.94.
  - [17] A.F. Martini, M.J. Menon and D.S. Thober, Phys. Rev. D **57**, 3026 (1998).
  - [18] A. Capella and J. Trần Thanh Vân, Phys. Lett. B **93**, 146 (1980); Z. Phys. C **20**, 249 (1981); Phys. Lett. B **114**, 450 (1982).
  - [19] Liu Lian-sou and Meng Ta-chung, Phys. Rev. D **27**, 2640 (1983); Chou Kuang-chao, Liu Lian-sou and Meng Ta-chung, Phys. Rev. D **28**, 1080 (1983); Cai Xu, Liu Lian-sou and Meng Ta-chung Phys. Rev. D **29**, 869 (1984).
  - [20] A.D. Martin and C. J. Maxwell, Z. Phys. C **34**, 71 (1987); S.G. Matinyan and W.D. Walker, Phys. Rev. D **59**, 034022 (1999).
  - [21] B. Andersson *et al.*, Phys Rep. **97**, 31 (1983); T. Sjostrand, Comp. Phys. Comm. **82**, 74 (1994); G. Schuler and T. Sjostrand, Phys. Rev. D **49**, 2257 (1994).
  - [22] G. Marchesini *et al.*, Comp. Phys. Comm. **67**, 465 (1992).
  - [23] L. Loennblad, Comp. Phys. Comm. **71**, 15 (1992).
  - [24] R. Henzi and P. Valin, Nucl. Phys. **B148**, 513 (1979).
  - [25] R. Henzi and P. Valin, Phys. Lett. B **132**, 443 (1983); B **160**, 167 (1985); B **164**, 411 (1985).
  - [26] R. Henzi and P. Valin, Z. Phys. C **27**, 351 (1985).
  - [27] DELPHI Collab., P. Abreu *et al.*, Z. Phys. C **50**, 185 (1991).
  - [28] Multiplicity distributions and average multiplicity in  $e^+e^-$  annihilations: TASSO Collab., W. Braunschweig *et al.*, Z. Phys. C **45**, 193 (1989); HRS Collab., M. Derrick *et al.*, Phys. Rev. D **34**, 3304 (1986); AMY Collab., H.W. Zheng *et al.*, Phys. Rev. D **42**, 737 (1990); OPAL Collab., G. Alexander *et al.*, Z. Phys. C **72**, 191 (1996); OPAL Collab., K. Ackerstaff *et al.*, Z. Phys. C **75**, 193 (1997).
  - [29] Average multiplicities in  $e^+e^-$  annihilations: MARK I Collab., J.L. Siegrist *et al.*, Phys. Rev. D **26**, 969 (1982); LENA Collab., B. Niczyporuk *et al.*, Z. Phys. C **9**, 1 (1981); JADE Collab., W. Bartel *et al.*, Z. Phys. C **20**, 187 (1983); MARK II Collab., G.S. Abrams *et al.*, Phys. Rev. Lett. D **64**, 1334 (1990); OPAL Collab., P.D. Acton *et al.*, Z. Phys. C **53**, 539 (1992); ALEPH Collab., D. Decamp *et al.*, Phys. Lett. B **234**, 209 (1990); DELPHI Collab., P. Abreu *et al.*, Phys. Lett. B **372**, 172 (1996); DELPHI Collab., P. Abreu *et al.*, Phys. Lett. B **416**, 233 (1998); DELPHI Collab., P. Abreu *et al.*,

- ICHEP'98 Conference, Vancouver, July 22-29 DELPHI 98-16 CONF 117.
- [30] R.E. Ansorge, in *Proceedings of the International Europhysics Conference on High Energy Physics*, edited by J. Guy and C. Costain (Rutherford Appleton Laboratory, Oxfordshire, UK, 1983) p. 268; P. Valin, Z. Phys. C **34**, 313 (1987).
  - [31] A. Wroblewski, Acta Physica Polonica, B **4**, 857 (1973).
  - [32] S. Rudaz and P. Valin, Phys. Rev. D **34**, 2025 (1986); D **35**, 2264 (1987).
  - [33] A. Breakstone *et al.*, (ABCDWH Collaboration), Phys. Rev. D **30**, 528 (1984).
  - [34] UA5 Collaboration, Phys. Rep. **154**, 250 (1987).
  - [35] M.J. Menon, in *Proceedings of the Fourth International Conference on Elastic and Diffractive Scattering* [2], p. 94; M.J. Menon and B.M. Pimentel, Hadronic J. **13**, 325 (1990).
  - [36] M.J. Menon, Can. J. Phys. **74**, 594 (1996).
  - [37] T.T. Chou and C.N. Yang, Phys. Rev. **175**, 1832 (1968); *ibid* **170**, 1591 (1968); Phys. Rev. Lett. **20**, 1213 (1968).
  - [38] T.T. Chou and C.N. Yang, Phys. Lett. B **244**, 113 (1990).
  - [39] S. Barshay and Y. Yamaguchi, Phys. Lett. B **51**, 376 (1974).
  - [40] E.L. Feinberg, Phys. Rep. **5**, 237 (1972); Sov. Phys. Usp. **26**, 1 (1983).
  - [41] E. Konish, T. Shibata, E.H. Shibuya, N. Tateyama, Prog. Theor. Phys. **56**, 1845 (1976).
  - [42] G. Wilk, in *Hadronic Multiparticle Production*, edited by P. Carruthers (World Scientific, Singapore, 1988) p. 410.
  - [43] P. Carruthers and M. Duong-Van, Phys. Lett. B **44**, 507 (1973).
  - [44] L. Criegge and G. Knies, Phys. Rep. **83**, 151 (1982).
  - [45] C. Berger *et al.*, Phys. Lett. B **95**, 313 (1980).
  - [46] G. Eilam and Y. Gell, Phys. Rev. D **10**, 3634 (1974).
  - [47] B. Margolis, P. Valin, M.M. Block, F. Halzen and R.S. Fletcher, Phys. Lett. B **213**, 221 (1988).
  - [48] P. L'Heureux, B. Margolis and P. Valin, Phys. Rev. D **32**, 1681 (1985); B. Margolis, P. Valin and M.M. Block, in *Proceedings of the Second International Conference on Elastic and Diffractive Scattering* [2], p. 277; B. Margolis and P. Valin, Can. J. Phys. **67**, 1101 (1989).
  - [49] R. Henzi, in *Proceedings of the First International Conference on Elastic and Diffractive Scattering* [2], p. 271.

## Figure Captions

Fig. 1. The KNO charged multiplicity distribution for  $e^+e^-$  annihilation data [27,28] and the fitted gamma distribution, Eq. (30) (dashed).

Fig. 2. The average charged multiplicity for  $e^+e^-$  annihilation data [28,29] and the fitted power law, Eq. (31).

Fig. 3. Scaled multiplicity distribution for inelastic  $pp$  data [33] at ISR energies compared to theoretical expectations using Eqs. (28-29).

Fig. 4. Scaled multiplicity distribution for inelastic  $\bar{p}p$  data [34] at 546 GeV compared to theoretical expectations using Eqs. (28-29) (solid) and predictions at 14 TeV (dashed).

Fig. 5. Inelastic overlap functions for  $\bar{p}p$  collisions at 546 GeV, predicted by the multiple diffraction model (MDM), geometrical model (GM) and the short-range-expansion, black-edge-large approach (BEL): (a) central region; (b) large distances.

Fig. 6. Same as Fig. 4 with the three different inputs for the inelastic overlap function. Same legend of Fig. 5.

Fig. 7. Same as Fig. 1 with the Barshay-Yamaguchi parametrization, Eq. (41).

Fig. 8. Same as Fig. 4 with two different inputs for the elementary multiplicity distributions: gamma function, Eq. (30) (solid) and Barshay-Yamaguchi parametrization, Eq. (41) (dot-dashed).

Fig. 9. Same as Fig. 2 with three power-law parametrizations:  $\gamma = 0.516$  (solid),  $\gamma = 0.500$  (dotted) and  $\gamma = 0.396$  (dot-dashed). In the last case only data above 10 GeV were fitted.

Fig. 10. Same as Fig. 4 using the three different parametrizations for the elementary average multiplicity (Fig. 9 and same legend).

Fig.1

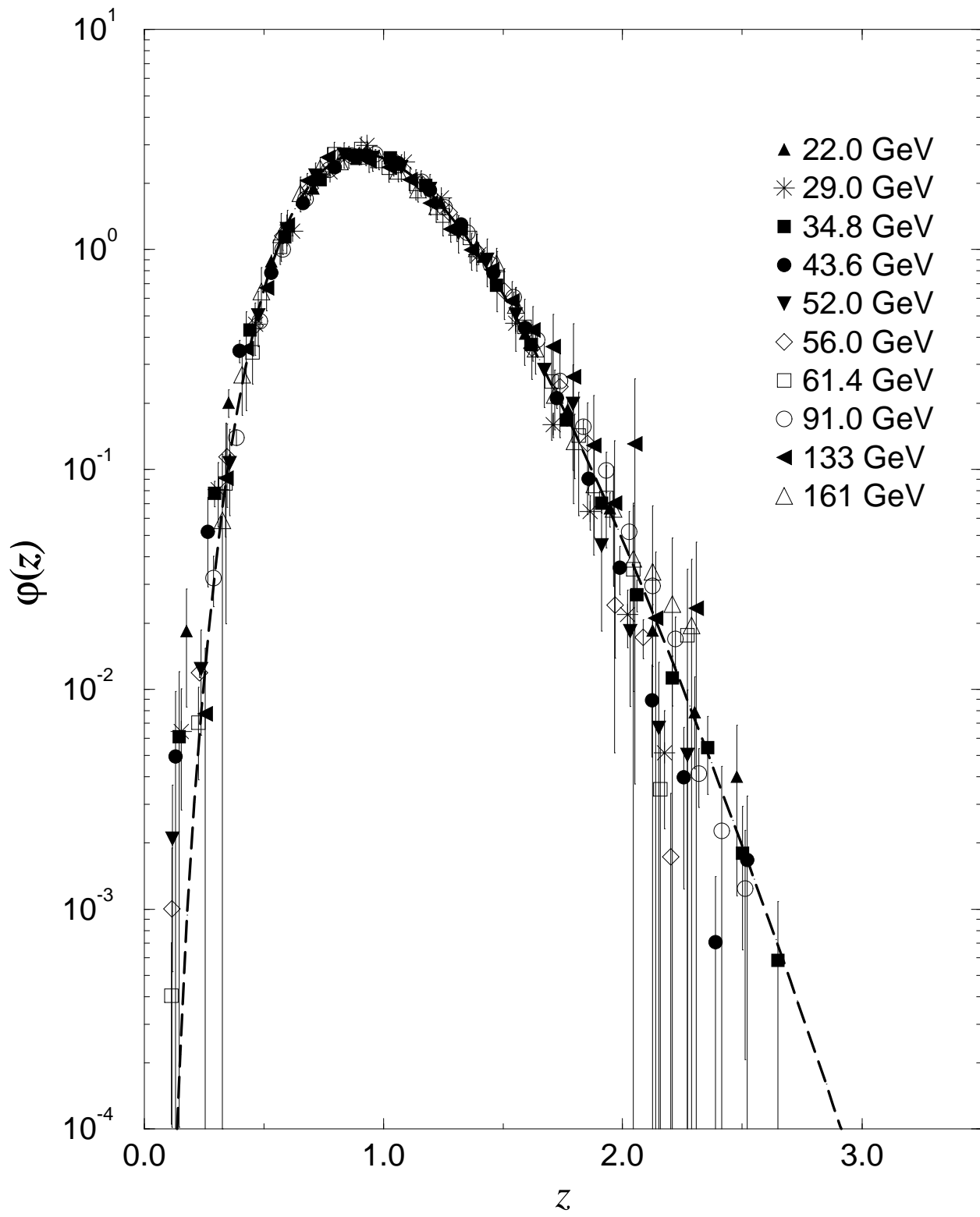


Fig.2

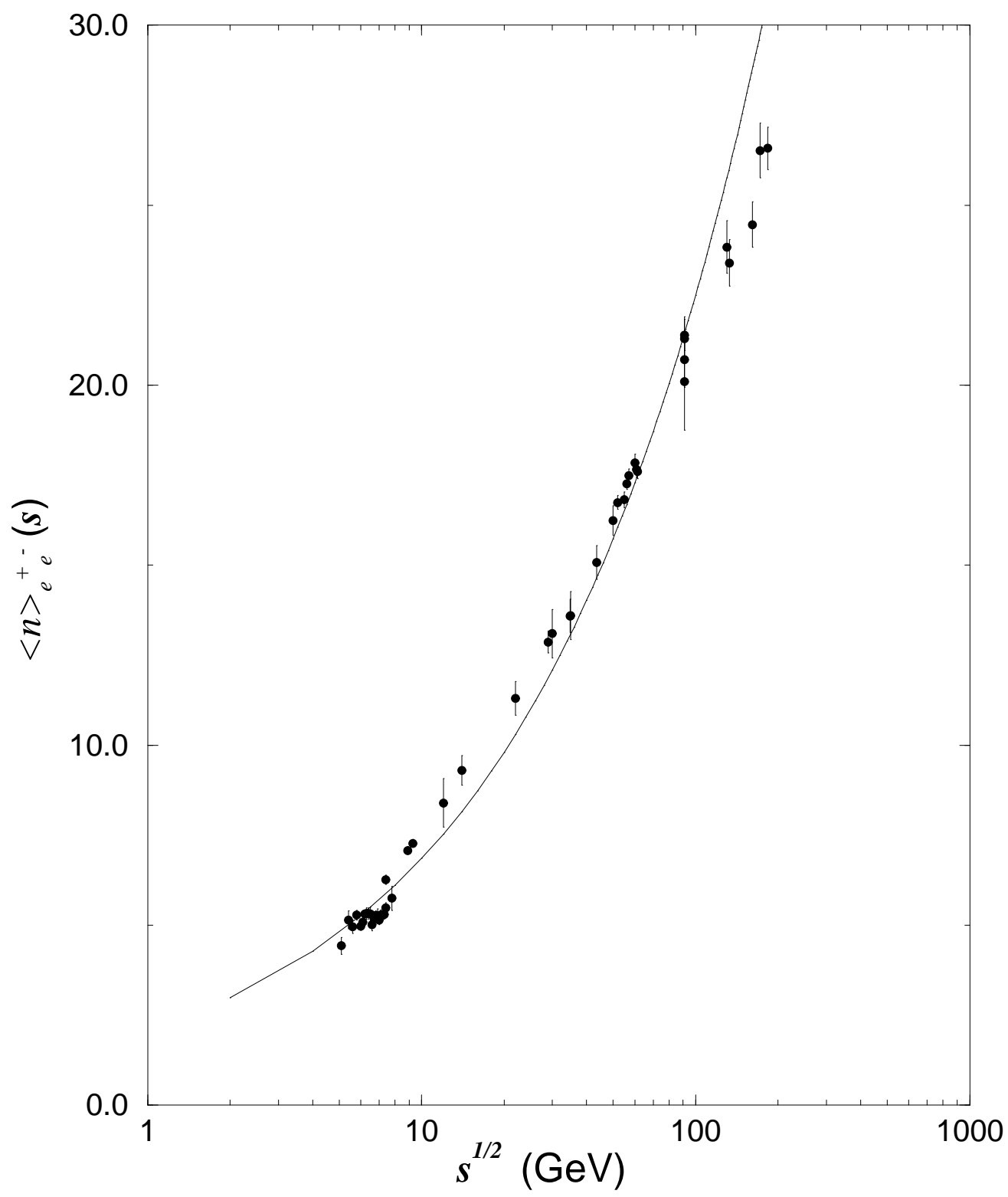


Fig.3

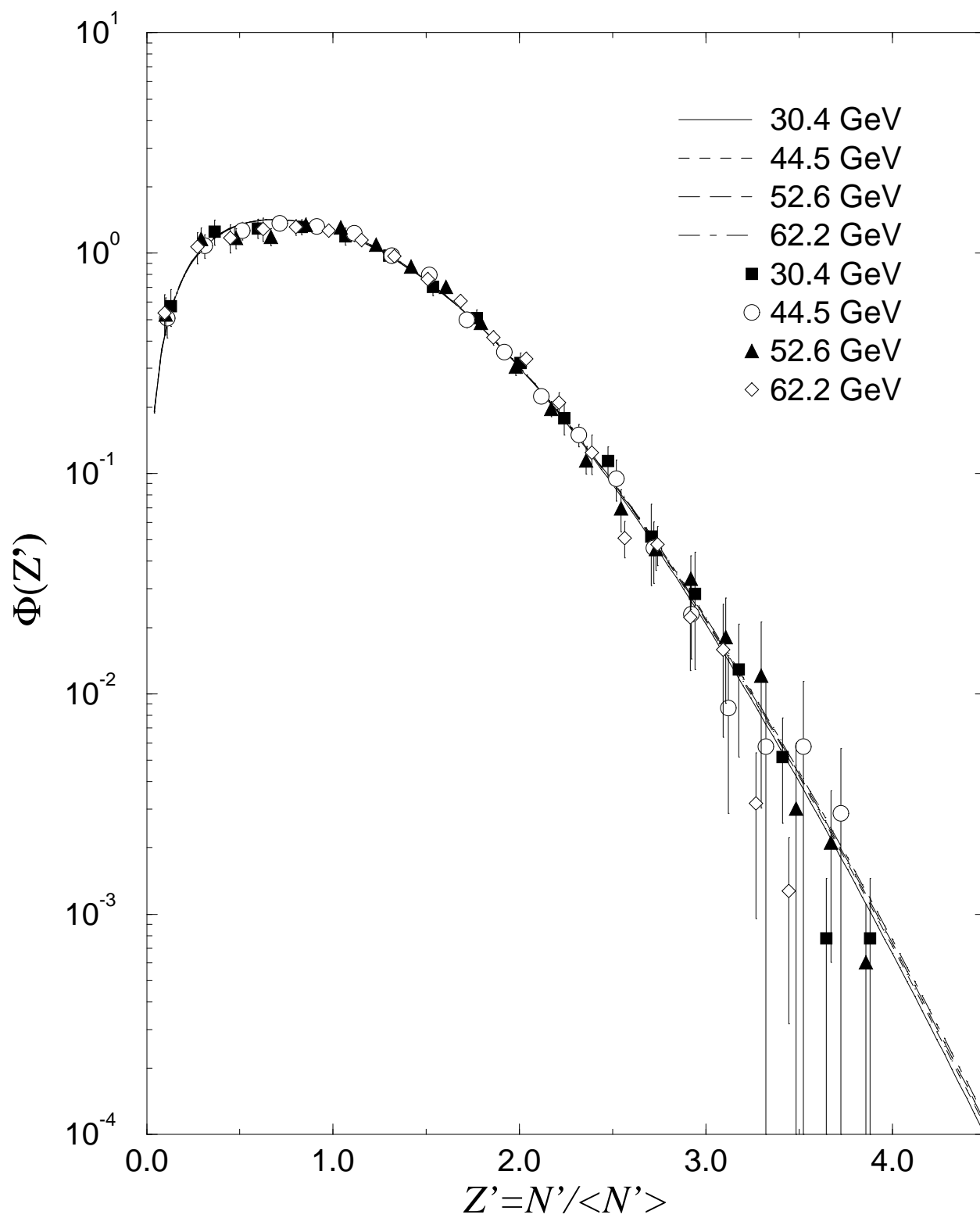


Fig.4

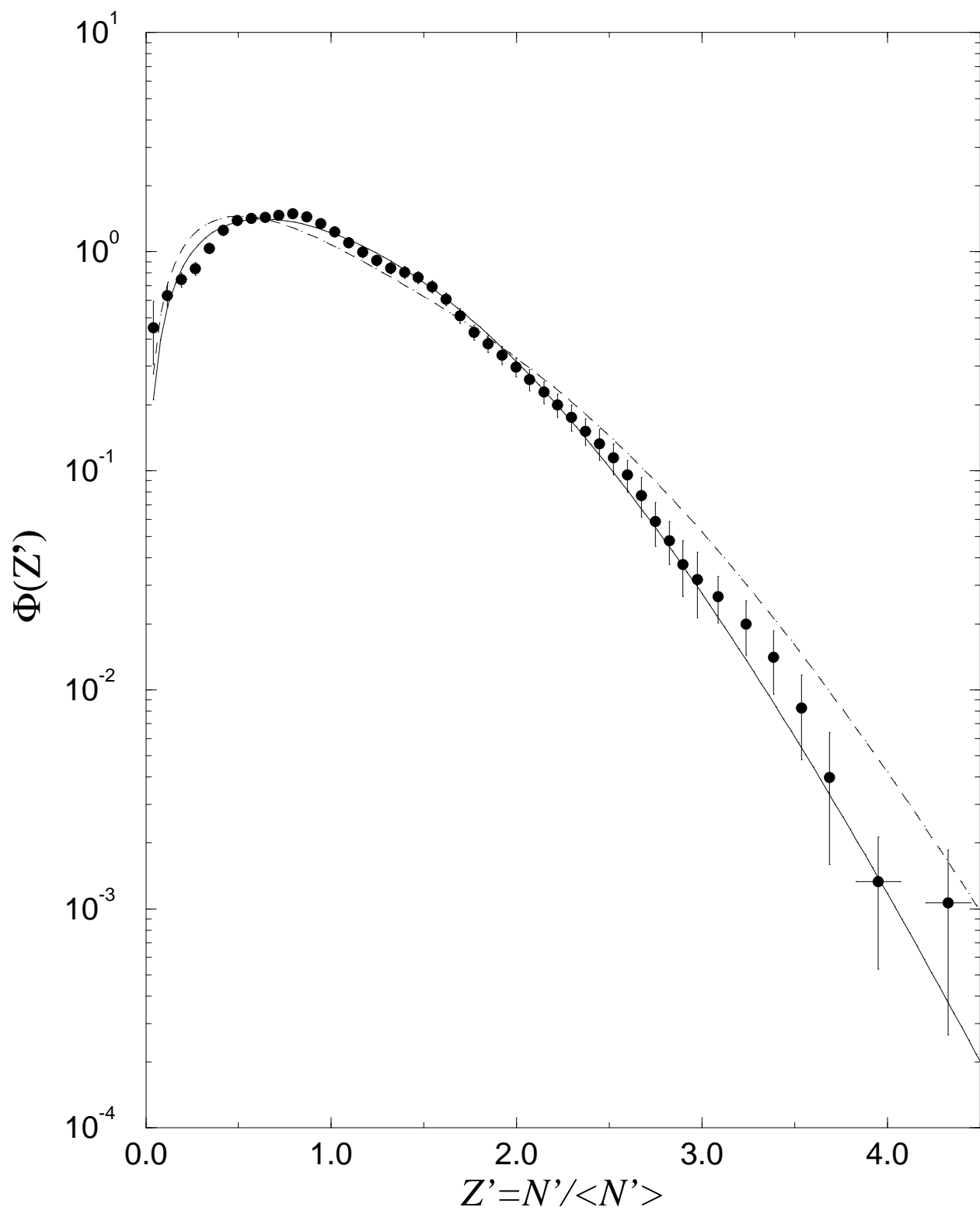


Fig.5a

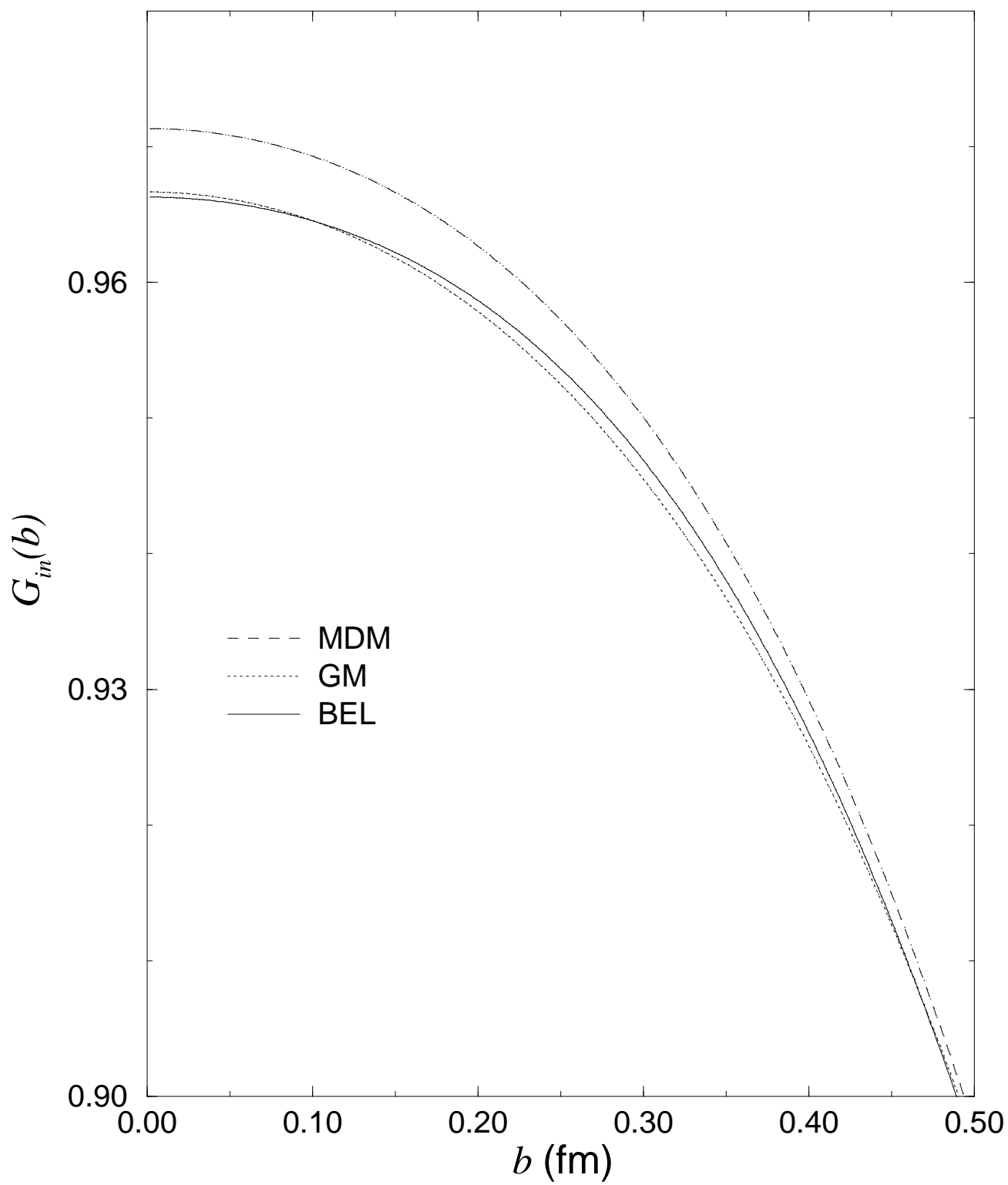


Fig.5b

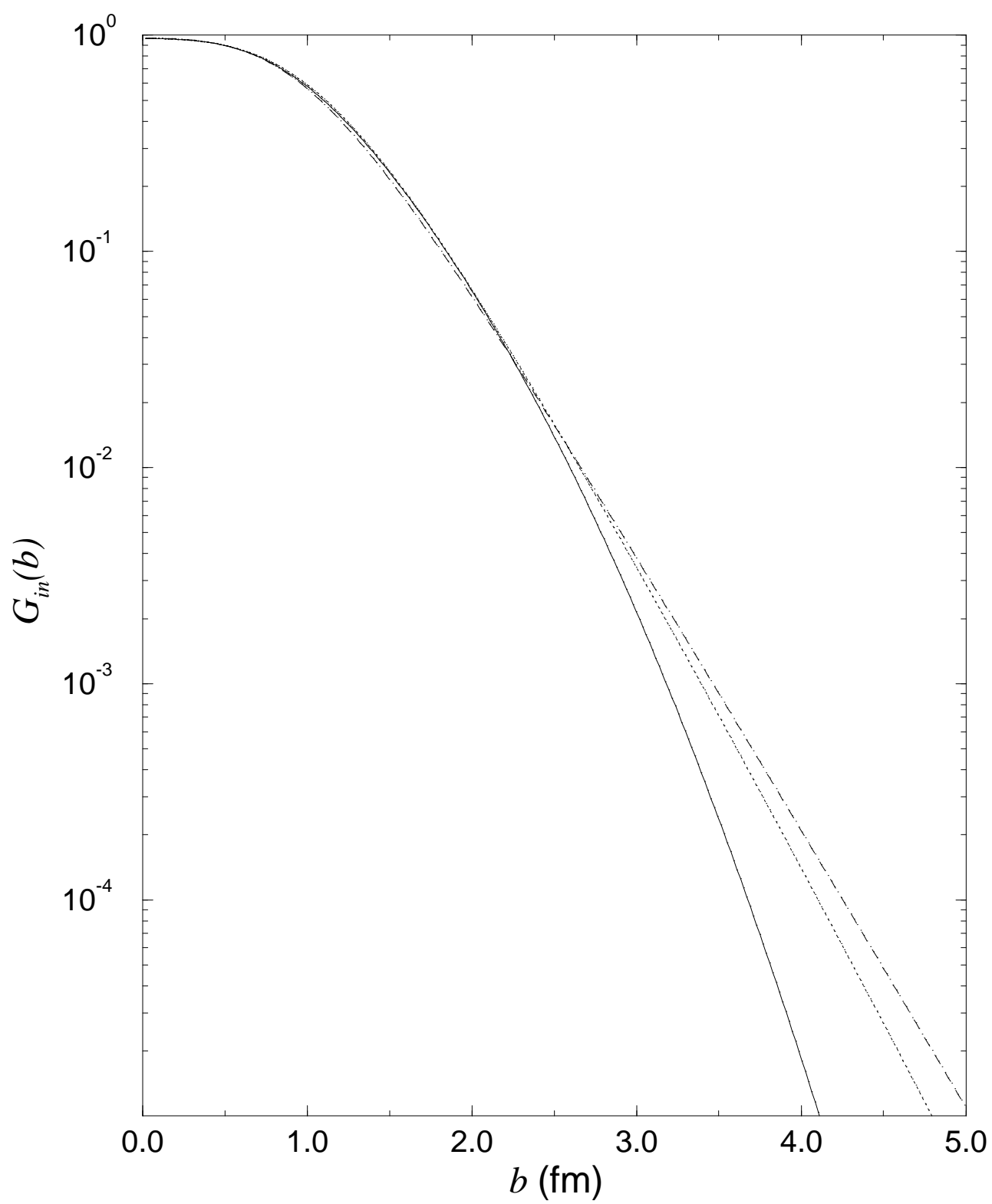


Fig.6

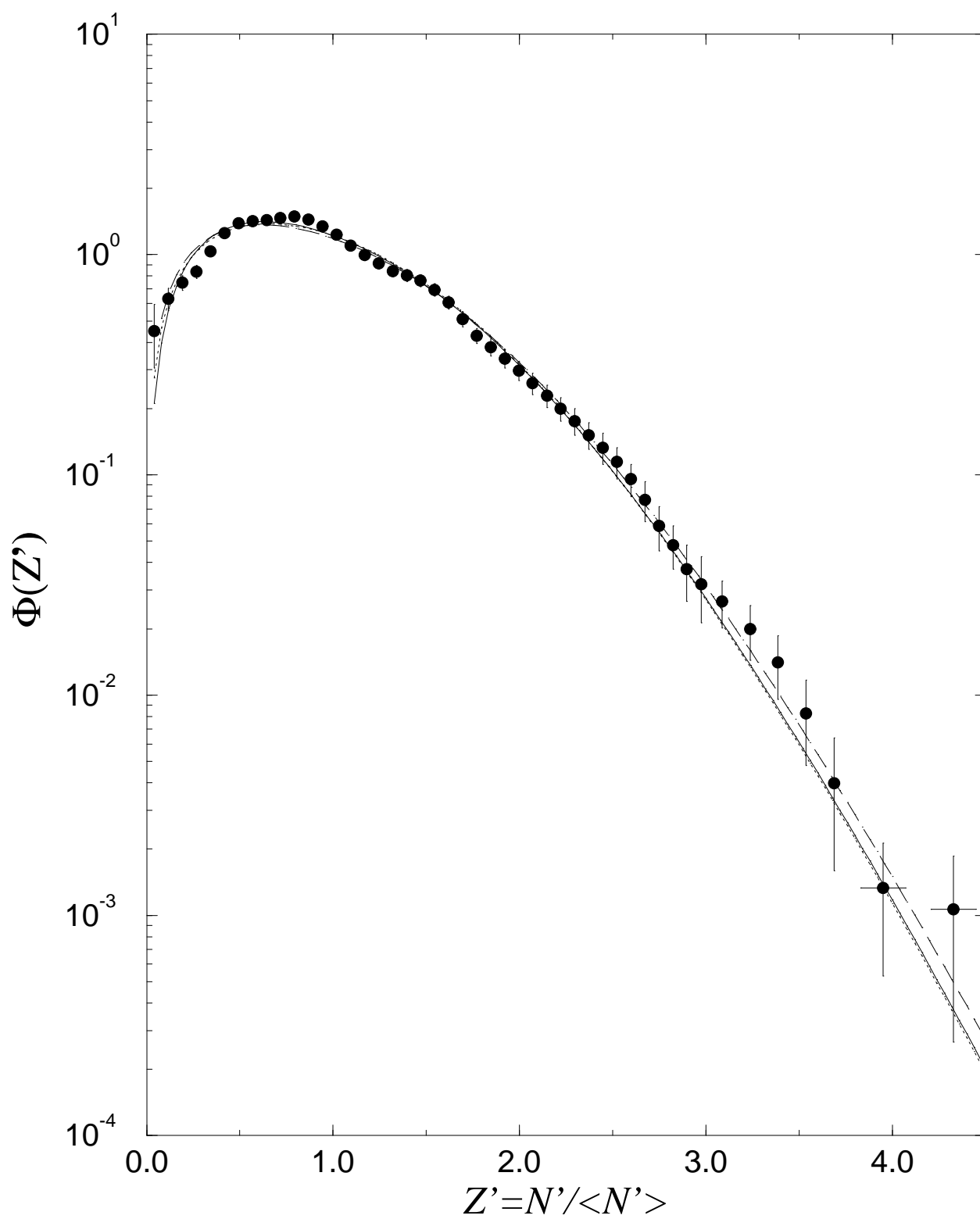


Fig.7

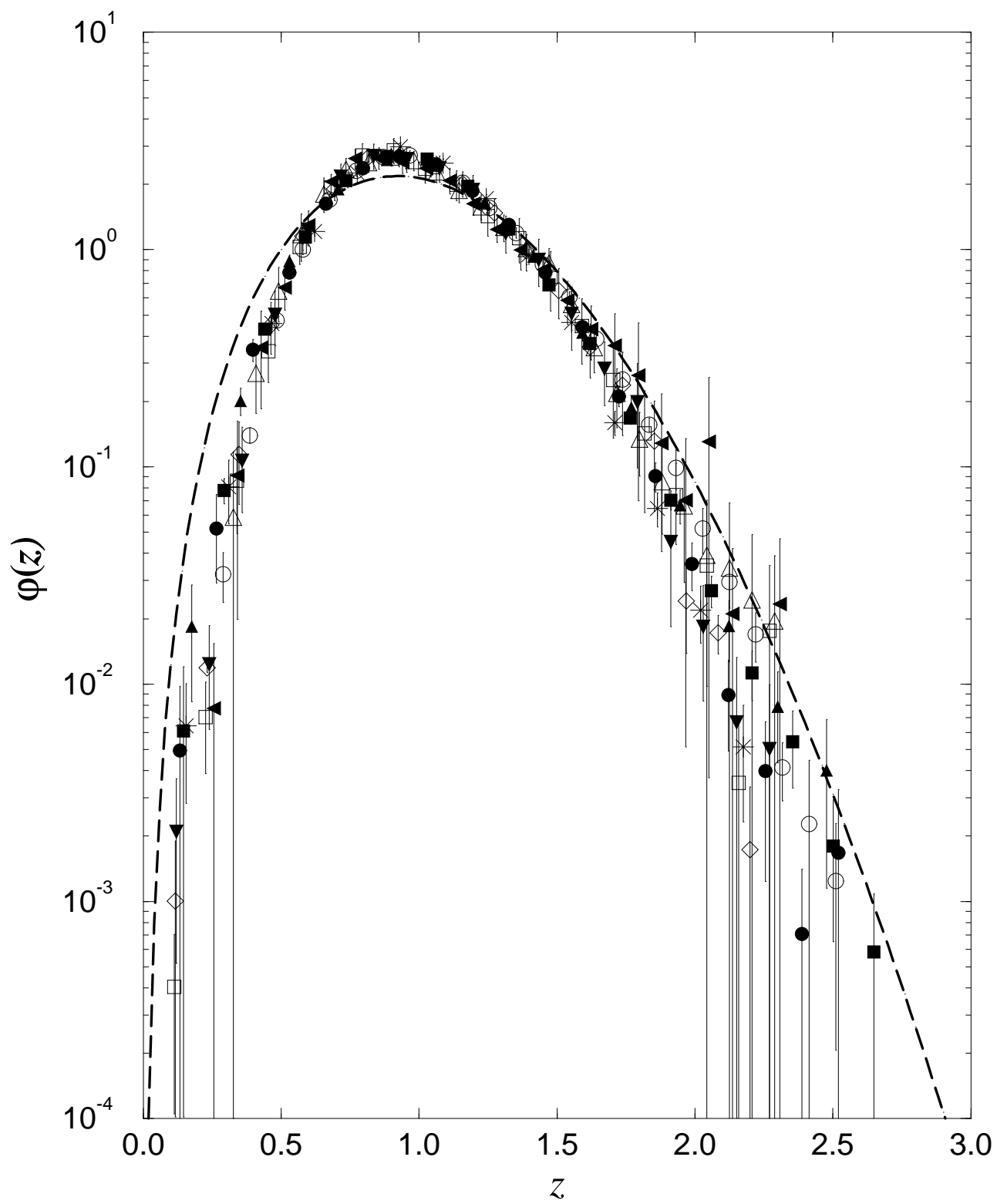


Fig.8

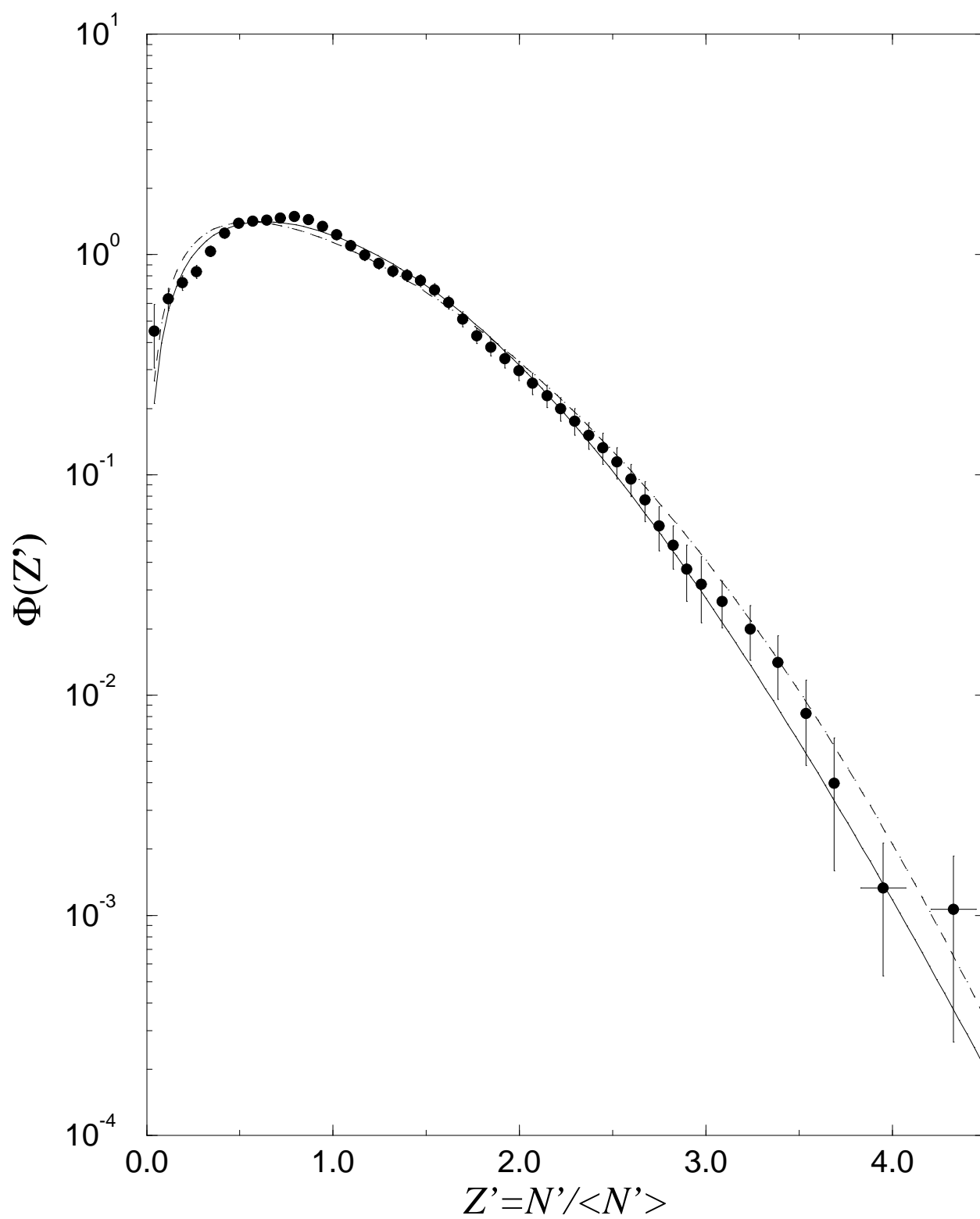


Fig.9

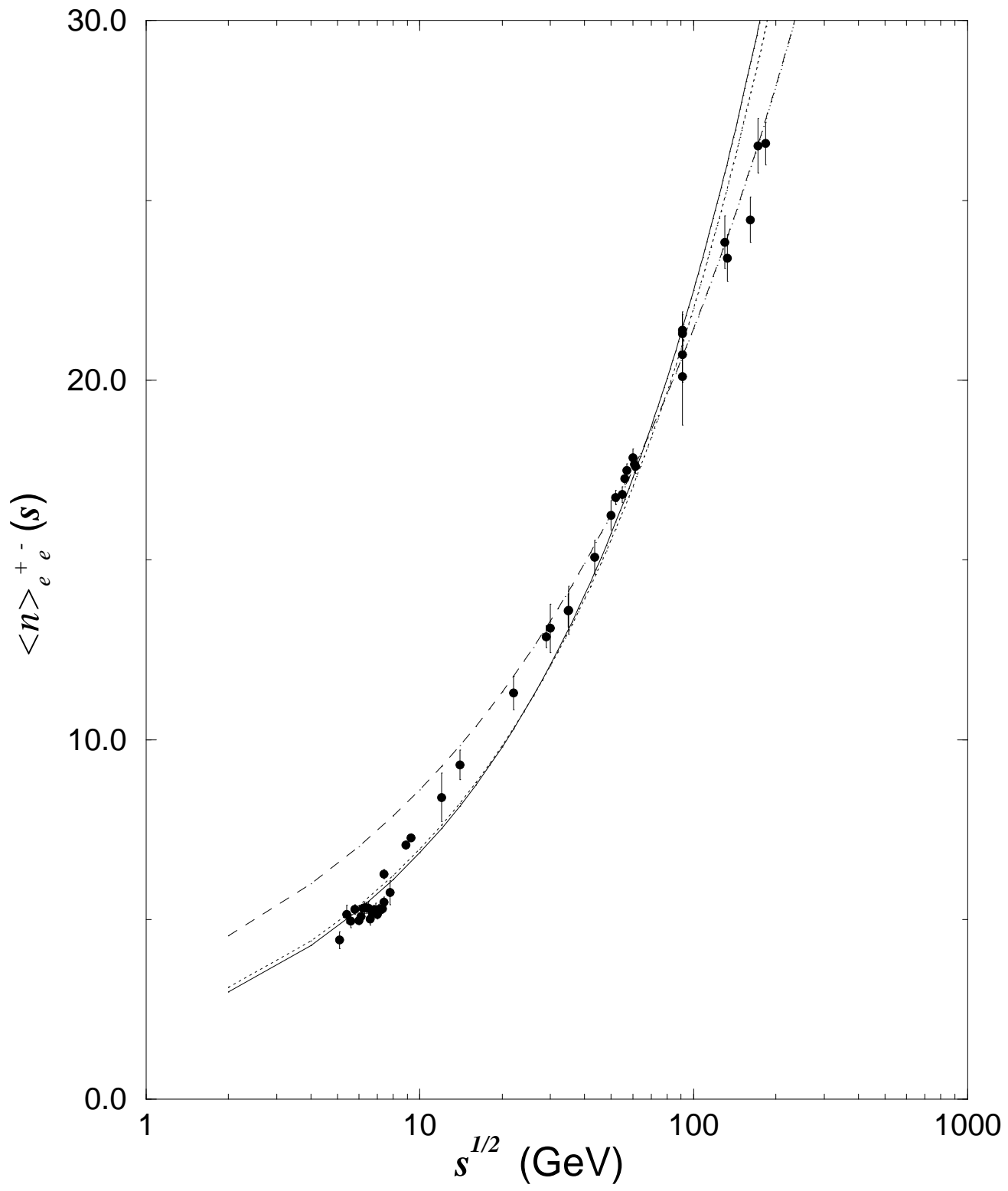


Fig.10

